

Mapping and Scheduling Spiking Neural Networks On Segmented Ladder Bus Architectures

Phu Khanh Huynh^a, Francky Catthoor^b, Anup Das^a

^aDepartment of Electrical and Computer Engineering, Drexel University, Philadelphia, 19104, PA, United States

^bNational Technical University of Athens, Athens, Greece

Abstract

Large-scale neuromorphic architectures consist of computing tiles that communicate spikes using a shared interconnect. The communication patterns in such systems are inherently sparse, asynchronous, and localized due to the spiking nature of neural events, characterized by temporal sparsity with occasional high bursts of traffic. These characteristics necessitate interconnects optimized for handling high-activity bursts while consuming minimal power during idle periods. Dynamic segmented bus has been proposed as one of the promising interconnects for such system for its simplicity, scalability and low power consumption. However, deploying spiking neural network applications on such buses presents challenges, including substantial inter-cluster traffic, which can lead to elevated network congestion and spike loss, as well as unnecessary energy expenditure. In this paper, we propose a three step process to deploy spiking neural network applications on dynamic segmented bus that aims to reduce spike loss and conserve energy. Firstly, we formulate optimization heuristics to mitigate spike loss and energy consumption based on application network connectivity. Secondly, we analyze the application traffic to determine spike schedule that minimize traffic flooding. Lastly, we propose a routing algorithm to minimize spike traffic path crossings. We then evaluate our approach using a cycle-accurate network simulator. The simulation results show that our mapping and scheduling algorithms can completely eliminate spike loss while keeping energy consumption much lower compared to conventional NoCs.

Keywords:

Segmented Bus, Ladder Bus, Neuromorphic Computing, Spiking Neural Networks, Optimization

1. Introduction

An event-driven neuromorphic system is a computing platform that implements biological neurons and synapses in hardware to execute spiking neural networks (SNN) [1]. To address design scalability, a neuromorphic system is designed as a many-core hardware, where cores are interconnected using a shared time-multiplexed interconnect such as shared bus, network-on-chip (NoC) (e.g., NorthPole [2], DYNAP-SE2 [3]), and segmented bus (e.g., μ Brain [4]).

The traffic in such systems is driven by spiking events, differing fundamentally from the continuous and synchronous communication typical of traditional computing architectures. A defining feature of neuromorphic traffic is temporal sparsity [5, 6]. Communication occurs only when a neuron generates a spike, resulting in sparse data traffic. In large-scale neuromorphic systems, densely connected neurons are typically grouped within the same clusters, while connections between clusters remain sparse. This clustering leads to traffic patterns where inter-cluster communication can experience short periods of intense activity, especially when many neurons spike simultaneously, followed by long periods of inactivity. Consequently, the communication infrastructure supporting neuromorphic system must be optimized to accommodate this characteristic: it must not only handle high-burst traffic efficiently but also consume minimal power during idle states.

Similar to other many-core architectures, SNN applications are required to be mapped to the hardware prior to execution. This process usually includes, but not limited to: partitioning the application into several clusters which can fit into the hardware neural core; placing the clusters into hardware based on the application connectivity; and scheduling/routing the spike traffic between cores. Previous works have been proposed to address mapping SNNs into neuromorphic hardware, such as SpiNeMap [7] and [8]. These works show that optimized mapping can greatly influence the performance of the running SNN application, including energy consumption, latency, and inter-spike interval.

However, these methods mainly perform such mapping operations on NoCs, which is not fully suitable for running SNN applications. The rationale for this can be attributed to the significant energy and area overhead of NoC, which is mainly due to the use of large buffers to temporarily store data packets and look-up tables (LUTs) to store routing tables inside each switch. While effective for conventional data handling, such design becomes resource-intensive in neuromorphic contexts where communication is sparse and irregular. A major factor contributing to this inefficiency is the leakage power associated with the substantial memory capacity required by the buffers. This results in unnecessary energy consumption, which contradicts the low-power and burst-like spike traffic requirements that are critical for neuromorphic systems. To mitigate such disadvan-

tages, bufferless NoCs have been proposed as an alternative to buffered NoCs [9]. However, in bufferless NoCs, when multiple packets compete for the same output port, all but one packet must be deflected and rerouted through alternative paths. This deflection process leads to additional traversals through the network [10], thereby increasing the overall network activity and energy consumption.

Segmented bus has been introduced as an alternative for NoC in these multi-core neuromorphic hardware systems. While the switches in a segmented bus are also bufferless, the communication system is structured to minimize path crossings, effectively avoiding the deflection and rerouting issues typically encountered in bufferless NoCs. It was shown that segmented buses such as NeuSB [11] outperforms NoCs in both latency and energy consumption for running SNN applications. Nevertheless, NeuSB lacks runtime switch controls and thus does not truly support running different applications on the same hardware. In this work, we focus on segmented ladder bus [12], the latest dynamic segmented bus interconnect that can offer runtime configuration for routing and scheduling network traffic.

We propose a mapping/scheduling framework, namely **MASS** (**MA**pping and **S**cheduling **SNN**s), that can fully deploy any SNN to segmented ladder bus architectures. Our main contributions for this paper are as follows:

- We propose a mapping algorithm based on Hill Climbing technique that can help minimize both energy consumption and spike loss in the network.
- We are the first to show a spike traffic scheduling and routing algorithms in dynamic segmented ladder bus.
- We evaluate our algorithms individually and combine to show the contribution of each step and prove that overall segmented ladder bus can indeed support large SNN applications while preserving energy consumption.

The remainder of the paper is organized as follows. A background introduction regarding dynamic segmented ladder bus and related mapping works are presented in Section 2. The overview of the proposed solutions and detailed algorithms are presented in Section 3. Evaluation methodology is presented in Section 4. Results and discussions are presented in Section 5. Finally, the paper is concluded in Section 6.

2. Background and Related Works

This section presents the requisite background to comprehend the segmented ladder bus [12], the primary interconnect architecture targeted by our mapping and scheduling methodologies. Furthermore, we review related works on the mapping of SNNs to neuromorphic hardware architectures, emphasizing the associated challenges and recent innovations in this domain.

2.1. Segmented Ladder Bus

The architecture of a segmented ladder bus is designed with the following characteristics:

- The tiles are logically divided into two parallel rows, each comprising an equal number of tiles.
- A fixed number of parallel segmented bus lanes are placed between these tile rows.
- The connections between the tiles and parallel bus lanes are established using criss-cross three-way switches.

A segmented ladder bus is governed globally by a compile time software framework and locally use coarse-grain runtime hardware controllers in order to enable dynamic configuration of switches. These local controllers encompass predefined switch change scenarios and facilitate the transmission of control signals to the switches accordingly. By issuing the control signals from the controllers with the correct timing, the switches can be used to create paths that support multiple simultaneous connections inside the network, matching application requirements. The controllers are implemented in a distributed manner, where each controller is responsible for managing the switches within its vicinity, similar to a distributed loop controller [13]. As a result, in a large-scale network, numerous controllers will be deployed to effectively govern the switches throughout the system.

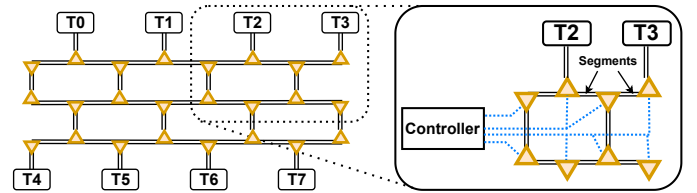


Figure 1: An example of segmented ladder bus with a switch controller.

Figure 1 illustrates an exemplary implementation of a segmented ladder bus comprising 8 tiles and 3 parallel segmented bus lanes. It is important to highlight that both the number of tiles and bus lanes can be scaled according to the specific requirements of the target application. This design framework offers several key advantages:

- **High Flexibility:** The network architecture facilitates communication between any pair of tiles within the system, ensuring robust interconnectivity.
- **Enhanced Routing and Fault-Tolerance:** Multiple distinct paths are available for communication between any two tiles, providing diverse routing options and improving the system's fault-tolerance capabilities.
- **Run-Time Configurability:** The switches can be configured during run time, allowing the segmented ladder bus to provide scheduling options under network congestion.
- **Energy and Area Efficiency:** The bufferless data plane significantly reduces energy consumption and minimizes the interconnect design area.

A more comprehensive understanding of the advantages offered by segmented ladder bus can be gained through an examination of Figure 2. Using the cluster communication graph

with a suitable mapping, multiple communication paths can be facilitated simultaneously: Tile 0 sends spikes to Tiles 5 and 6, Tile 1 sends to Tile 2, and Tile 7 to Tiles 3 and 8.

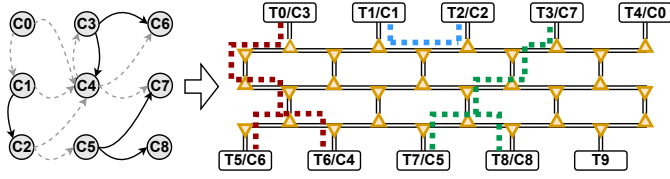


Figure 2: Multiple routing options in a segmented ladder bus

2.2. Related Works

Mapping neuromorphic clusters to hardware cores in network-on-chip (NoC) architectures has garnered significant attention in recent years due to its potential to enhance the performance and efficiency of neuromorphic computing systems. Several notable approaches and frameworks have been proposed to address this challenge.

One prominent method is SpiNeMap [7], which focuses on optimizing the mapping of spiking neural networks (SNNs) onto neuromorphic hardware. SpiNeMap employs a multi-objective optimization strategy to balance energy consumption, latency, and inter-spike interval. By considering the unique communication patterns and computational requirements of SNNs, SpiNeMap achieves significant improvements in the overall performance of neuromorphic systems. Similarly, SNEAP [14] suggested using one of the three heuristics, namely Simulated Annealing, Particle Swarm Optimization, and Tabu search for mapping neuromorphic clusters to NoC. However, their reliance on static NoC topologies limits its scalability and adaptability to dynamic workloads.

Another approach by Jin et al. [8] presents a heuristic-based mapping algorithm that aims to minimize communication overhead in NoC-based neuromorphic systems. It solves the initial placement using the Hilbert curve, a space-filling curve with unique properties that are particularly suitable for mapping SNNs. Afterwards, a Force Directed algorithm is developed to optimize the initial placement. This method leverages the inherent sparsity of SNNs to reduce the number of active communication channels, thereby lowering energy consumption and improving latency. Despite its effectiveness, the heuristic nature of this algorithm may not always guarantee optimal mappings, especially in larger and more complex networks.

NeuMap [15] introduces a machine learning-based technique for mapping neuromorphic clusters on NoC architectures. By training a neural network to predict optimal mappings based on historical data, NeuMap can dynamically adjust to varying workloads and network conditions. This adaptive approach demonstrates significant potential in enhancing the efficiency of neuromorphic systems. Nonetheless, the training overhead and the need for extensive historical data may pose challenges in real-time applications.

In summary, the field of mapping neuromorphic clusters onto interconnect architectures is abundant with innovative approaches and significant advancements. However, existing approaches primarily target NoCs and fail to address the

unique challenges associated with mapping applications onto segmented bus-based neuromorphic hardware. Therefore, there is a significant need for more tailored and efficient techniques for mapping, scheduling, and routing neuromorphic clusters on segmented ladder bus architectures.

3. Proposed Solutions

In our previous work [16], we have described the SNN application partitioning process in more details. This allocates neurons to memristive crossbar clusters while maximizing the crossbar utilization and minimizing inter-cluster communication. Although such process is essential, it works independently of the types of interconnect hardware. For this reason, it is not the focus of this paper.

Once an SNN application has been partitioned into clusters, we need to: map the clusters to actual hardware tiles; schedule spike traffic; and route the scheduled traffic. Each of these steps can be optimized to improve the hardware utilization of the network, guarantee performance of the application, and reduce energy consumption. Figure 3 shows our proposed solution processes integrated inside our evaluation framework. While numerous state-of-the-art network simulators provide support for Network on Chip architectures, none currently offer built-in capabilities for simulating segmented bus architectures. Thus, we developed a custom network simulator tailored to segmented buses based on Noxim [17]. Noxim was chosen as the foundation for our simulator due to its open-source, extensible code-base, SystemC-based [18] cycle-accurate simulation engine, and lightweight, scalable design.

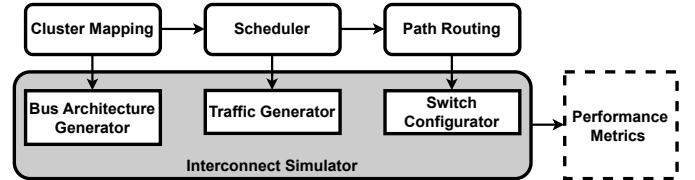


Figure 3: MASS design flow.

3.1. Cluster Mapping

After an SNN application has been partitioned into clusters, it is important to map these clusters into actual hardware tiles. The connectivity between the clusters can be represented as a directed graph $G_{CSNN} = (C, L)$ consisting of C clusters and L links between the clusters. A link $L_{i,j} \in L$ is a channel connecting cluster C_i with cluster C_j , where $C_i, C_j \in C$. Each link $L_{i,j}$ has a weight $s_{i,j}$ that represents the number of spikes communicated on $L_{i,j}$. A spike link activity indicator $z_{i,j} = 1$ if $s_{i,j} > 0$ and $s_{i,j} = 0$ otherwise. The cluster mapping problem can be modeled as an injective function ϕ that place the neuron clusters C into hardware tiles T .

Different mappings will have different impacts on energy consumption, latency, and the number of crossed communication paths. In our segmented ladder bus design, communication

energy consumption is proportional to the length of the communication paths and the number of switch configurations that need to be changed. Furthermore, unlike NoCs, the bufferless nature of the switches in segmented bus causes simultaneous intersecting communication paths to result in either packet drops or additional delays at the source nodes to avoid packet loss. Thus, we propose two different mapping cost functions specifically adapted to ladder segmented bus to minimize either dynamic energy consumption or number of crossed paths. They are computed as follows.

1. *Dynamic Energy*:

$$E = \sum_{i,j \in \{0,1,\dots,|C|\}} s_{i,j} \times d_{\phi(i),\phi(j)} \quad (1)$$

where $d_{\phi(i),\phi(j)}$ is the number of segments between the tiles that C_i, C_j are mapped to.

2. *Weighted crossed paths*: Since our interconnect architecture is completely bufferless, we need to find the maximum number of simultaneous connections to prevent spike loss and minimize the number of switching in the network. Although ladder segmented bus can support multicasting, it is important to note that this work focuses on unicast communication, and the extension to multicast scenarios is left for future work.

$$W = \sum_{i,j,k,l \in \{1,\dots,C\}} (s_{i,j} + s_{k,l}) \times z_{i,j} \times z_{k,l} \times \text{crossed}(\phi(L_{i,j}), \phi(L_{k,l})) \quad (2)$$

where $\text{crossed}(\phi(L_m), \phi(L_n))$ is the function to check whether a mapping would make the links L_m and L_n topographically cross each other (see Figure 4).

One can then select or combine the desired cost function depends on the application requirements, expressed as follows:

$$\text{Cost} = \alpha \times E + \beta \times W \quad (3)$$

where α and β are adjustable parameters.

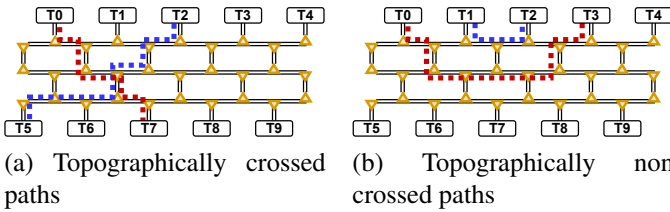


Figure 4: Example of topographically crossing.

Given that cluster mapping is a well-established NP-hard problem [19], a practical solution is implemented using a Hill Climbing approach [20]. This metaheuristic provides an efficient and practical way to explore the vast solution space while balancing computational cost and solution quality. We employ a specific variant, called steepest ascent Hill Climbing, to enhance the search process. The algorithm starts with a random mapping solution and compares the cost of that solution with

all neighboring solutions. A neighbor is defined as a mapping obtained by swapping the positions of two nodes in the current mapping. This ensures that the search space of the algorithm is limited to only valid mappings, which improve the efficiency of the search. The algorithm moves the solution to the neighbor with the most improved cost. The search continues until there is no neighbor with improved cost. The local search ends here, with the algorithm keeping record of this solution. It is important to note that Hill Climbing may converge to a local minima. To mitigate this, when the search terminates due to the lack of better-cost neighbors, we incorporate a number of random swaps and re-initiate the search procedure. Ultimately, the algorithm concludes its execution after running a predetermined number of random perturbations.

Algorithm 1: Cluster mapping algorithm.

Input: G_{CSNN}, η, I
Output: Mapping $\phi: C \rightarrow T$

```

1  $\phi_{best} = \text{random\_map}(C, T);$ 
2 for  $i = 1$  to  $\eta$  do /* loop over the number of perturbations */
3    $\phi_{current} = \text{random\_map}(C, T);$  /* generate random mapping */
4    $\phi_i = \phi_{current};$  /* set best local mapping to the current mapping */
5    $\text{improved} = \text{true};$ 
6    $k = 0;$ 
7   while  $\text{improved}$  and  $k < I$  do /* while cost is improved and under the number of iteration limit */
8      $k = k + 1;$ 
9      $\text{improved} = \text{false};$ 
10     $\text{change}_{best} = +\infty;$ 
11    for  $\phi_n \in \phi_{current}.\text{neighbours}()$  do /* iterate over all neighbours */
12       $\text{change} = \text{cost}(\phi_n) - \text{cost}(\phi_{current});$  /* compare the cost of current mapping and its neighbour */
13      if  $\text{change} < \text{change}_{best}$  then /* if the change of cost is lower than the best change */
14         $\text{change}_{best} = \text{change};$ 
15         $\phi_i = \phi_n;$  /* set best local mapping to the neighbour mapping */
16      end
17    end
18    if  $\text{change}_{best} < 0$  then
19       $\phi_{current} = \phi_i;$  /* move current mapping to the best neighbour cost mapping */
20       $\text{improved} = \text{true};$  /* set improvement flag if cost change in the right direction */
21    end
22  end
23  if  $\text{cost}(\phi_i) < \text{cost}(\phi_{best})$  then /* if cost of best local mapping is lower */
24     $\phi_{best} = \phi_i;$  /* set best global mapping to best local mapping */
25  end
26 end
27 return  $\phi_{best}$ 

```

Time Complexity Analysis: The time complexity of Algorithm 1 is computed as follows. A mapping of C clusters to T hardware nodes has a total of T^2 neighbours. For each local search, the number of iteration is limited to I , which in our experiments is set proportional to the number of tiles T . If the maximum allowed number of perturbation is η the overall time complexity is: $O(\eta T^3) \cdot O(\text{cost})$.

- The weighted crossed path cost function evaluates crossings between every pair of links. With L links, this results in L^2 crossings, leading to a time complexity of $O(\eta T^3 L^2)$.
- For the dynamic energy cost function, it calculates the

weighted sum across all L links. The resulting time complexity is $O(\eta T^3 L)$.

This polynomial complexity is manageable, as the mapping is performed only once at compile time.

3.2. Spike Traffic Scheduling

Despite efforts to minimize crossings between communication paths through our cluster mapping algorithm, the high density and frequency of application connectivity can occasionally prevent simultaneous facilitation of all required communication links. If the number of required simultaneous communication links exceeds the network's capacity, it can result in spike loss due to the bufferless nature of our architecture. Hence, it becomes necessary to schedule spike traffic to maintain application performance.

With the cluster mapping acquired from algorithm 1 and the spike traffic from CARLSim [21] or SNNTorh [22], we can obtain the exact timing of the spike traffic among the hardware tiles. For any given time with multiple simultaneous communication links, the scheduler would need to find groups of links for which no two links in any group intersect, while minimizing the number of groups to prevent unnecessary delays.

This problem is essentially a bin packing problem with conflicts (BPPC) [23], which is NP-complete. Therefore, instead of seeking an optimal schedule, we develop a custom heuristic to get a solution within a practical computational limit. An example of a spike traffic schedule can be found in Figure 5.

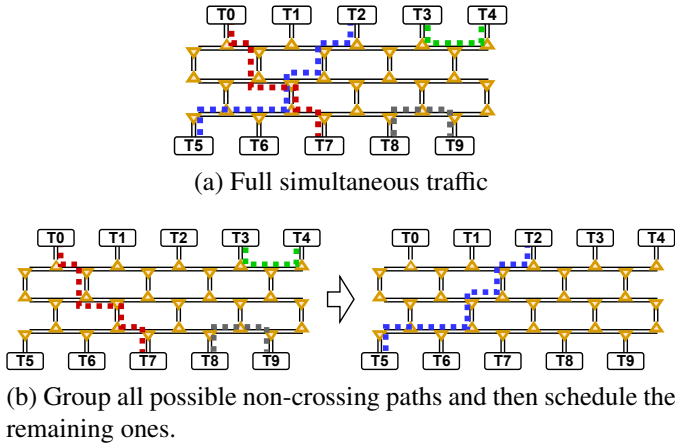


Figure 5: Example of scheduling traffic.

Heuristic Solution: The exact timing of the spike traffic among hardware tiles is denoted as T_O . We then iterate over all the traffic time steps in T_O . When multiple communication links need to run at the same time step, they are sorted according to the number of spikes communicated. We subsequently go through the sorted list, and attempt to group links that can operate concurrently without their paths intersect. Links in the same group can be scheduled to run at the same time. If a link intersects with any other link, a new group is formed with an additional delay for that group. This intersection check is based on the graph representation of the ladder bus G_{ladder} . Note that this check can be done using topological crossing or shortest

path crossing of links. The utilization of bus lanes is also taken into account when grouping the communication links. If adding a new link exceeds the available bus lane capacity, it is treated as intersecting with other links in the group. This process continues until all links are grouped with specific run times, ensuring that there are no intersections within any group. This scheduling process can be performed without affecting the application performance because the speed of the bus is much faster than the communication frequency of the neuron spikes.

Algorithm 2: Spike traffic scheduling algorithm.

```

Input:  $G_{ladder}, T_O$ 
Output: Scheduler
1 Scheduler =  $\emptyset$ ;
2 for time_step  $\in T_O$  do /* iterate over all traffic time steps */
3   SortedLinks = sort( $T_O$ [time_step]); /* sort the links in each
   time step */
4   TimeGroups =  $\emptyset$ ; /* create a list of groups for the current
   time step */
5   for  $L \in$  SortedLinks do /* go through all the links in the
   sorted link list */
6     added = False;
7     for Group  $\in$  TimeGroups do /* for each group in the
   current time step */
8       crossed = False;
9       for  $L_G \in$  Group do /* for each link in the group */
10        if check_cross( $G_{ladder}, L, L_G$ ) then /* check whether
   the current link L crosses with  $L_G$  */
11          crossed = True;
12        end
13      end
14      if crossed == False then /* if link L does not cross
   any link in the group */
15        Group.append(L); /* add link L to the group */
16        added = True; /* mark link L as added */
17      end
18    end
19    if added == False then /* if link L has not been added to
   any group */
20      TimeGroups.append(Set(L)); /* create a new group for
   L and add it to the list of groups */
21    end
22  end
23  delay = 0;
24  for Group  $\in$  TimeGroups do /* for each group in the current
   time step */
25    max_spike = 0;
26    for  $L_G \in$  Group do /* for each link in the group */
27       $L_G.time = time\_step + delay$ ; /* increase scheduled time
   of the link by the delay amount */
28      if max_spike <  $L_G.spikes$  then
29        max_spike =  $L_G.spikes$ ; /* find the maximum
   spikes sent in the group */
30      end
31    end
32    delay = delay + (max_spike  $\times$  N); /* increase the delay
   proportionally to the maximum spikes sent */
33  end
34  Scheduler.append(TimeGroups); /* add the list of groups to
   the scheduler */
35 end
36 return Scheduler

```

Time Complexity Analysis:

- For each time step, the links are sorted. Complexity of sorting L simultaneous links: $O(L \log L)$.
- For each link L , the algorithm checks existing groups to see if the link can be added without conflict. For each group, the algorithm checks if the new link crosses with any existing link in the group. This involves iterating over each link in the group, and for each pair of links, the check_cross

function is called, which can be simplified to take constant time $O(1)$ due to the defined and regular topology of the network. In the worst case, each link will be compared to all other $L - 1$ links, giving $O(L^2)$ comparisons.

- The delay adding steps from line 23 to line 33 just passes through the full list of links, thus has $O(L)$ running time.
- Hence, the scheduling complexity per time step is $O(L^2)$.

3.3. Path Routing

Once the scheduling process has been completed, the next crucial step is to perform routing of all the simultaneous connections. Efficient routing is essential to optimize the interconnect performance, and reduce unnecessary delays while still maintaining the maximal number of simultaneous connections.

Our solution to the path routing problem primarily adopts a greedy algorithm, supplemented by A* [24] sub-processes for efficient shortest path finding. We sort all the simultaneous communication links $CLinks$ according to the following order: we prioritize all the links with source and destination tiles on the same bus lane first, followed by sorting based on the orientation of the links, and finally by the number of spikes on each link. The reasoning of this sort is three folds: Firstly, we reduce the number of potential crossing between links by routing the links with source and destination tiles on the same bus lane and the shorter distance ones first. This is because the shortest path for tiles on the same bus lane is unique, while there can be many paths with the same length for tiles on different bus lanes. Secondly, links with the same orientation can be easily routed one by one so that they do not cross each other. Thirdly, by prioritizing to route the links with more spikes, the paths for these links will be shorter, which means lowering the number of spikes that need to travel long distances, which in turn helps in reducing the energy consumption in the network. We then represent the segmented ladder bus interconnect as an undirected graph G_{ladder} with tiles and switches as vertices and bus wires as edges. The initial weights of all vertices and edges in the graph are set to 1. The algorithm processes the sorted communication links sequentially, and uses a modified A* algorithm to determine the shortest weighted path for each specific link. After determining the shortest path for the selected link, the weights of all vertices are increased proportionally to the number of spikes communicated on this particular link. Subsequently, the routed link is removed from the list of communication links. The algorithm continues the process iteratively, selecting and routing the most communicated links one by one, until all paths are effectively routed.

Time Complexity Analysis: The time complexity of Algorithm 3 is computed as follows. Sorting L communication links takes $O(L \log L)$ time. In worst case scenario, A* algorithm takes $O(|E| + |V|)$ time where E and V are both proportional to the number of tiles T and bus lanes n in our architecture. We need to perform A* for L links. Thus, the overall time complexity is $O(nLT)$.

Algorithm 3: Path routing algorithm.

Input: $G_{ladder}, CLinks$
Output: $RoutedList$

```

1  $SLinks = sort(CLinks);$  /* sort the communication links */
2  $RoutedList = \emptyset;$ 
3 for  $L_{i,j} \in SLinks$  do /* each link in the sorted link list */
4    $Path = A\_star(i, j);$  /* find the path for the link using A* */
5   for  $node \in Path$  do /* for every node in the path */
6      $node.weight = node.weight + L_{i,j}.spikes;$  /* increase the
7       weight of the node by the number of spikes on the
8       link */
9   end
10   $RoutedList.add(Path);$  /* add the path to the routed list */
11 end
12 return  $RoutedList$ 

```

4. Evaluation Methodology

4.1. Benchmarks

Table 1 reports the machine learning applications utilized in the assessment of mapping SNNs into MASS. In each instance, a pruning methodology is employed to eliminate weights close to zero. For each model, we provide detailed information on the total number of clusters generated to run the application. Empirically, the number of bus lanes allocated per application is set to approximately the square root of the total number of clusters.

Application	# Clusters	Avg. Degree	Network Density	# Bus Lanes
mnist	12	1.50	0.27	4
LeNet	14	2.93	0.45	4
fashion-mnist [25]	24	5.33	0.46	5
cifar10	25	5.44	0.45	5
emnist [26]	30	5.37	0.37	6
ResNet [27]	96	11.13	0.23	10

Table 1: Applications used to evaluate our mapping and scheduling approaches.

4.2. Evaluation Approaches

We evaluate the following approaches.

- **ADIONA** or **MASS-SL** (Spike Loss): This baseline approach, previously used in ADIONA, focuses on mapping with the goal of reducing spike loss, without scheduling, and utilizes simple shortest path routing.
- **MASS-DE** (Dynamic Energy): This approach emphasizes mapping to minimize dynamic energy consumption, without scheduling, and also uses simple shortest path routing.
- **MASS-TXS** (Topological Crossing Schedule): This approach builds on MASS-SL by adding scheduling with a topological crossing check, while still applying simple shortest path routing.
- **MASS-SPXS** (Shortest Path Crossing Schedule): This approach is based on MASS-SL, incorporating scheduling with a shortest path crossing check, and also employs shortest path routing.
- **MASS-SR** (Sorted Routing): This approach is based on MASS-TXS with scheduling using topological crossing check, and uses our custom routing algorithm with sorted communication links.

5. Results and Discussions

5.1. Cluster mapping

In this experiment, we evaluate our mapping algorithm for optimizing both spike losses and energy consumption against random mappings obtained from 50 to 250 Monte Carlo simulations. Figure 6 plots the spike loss ratio for different mappings on the benchmark applications.

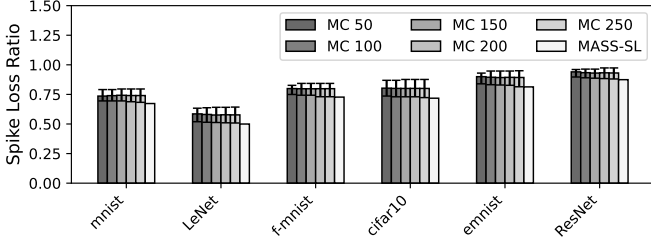


Figure 6: Spike loss ratio for different mappings.

On average, spike loss using our mapping algorithm and cost function is reduced by 10% compared to the average values founded using Monte Carlo method. Our mapping has lower spike loss percentage than the minimum values founded using Monte Carlo method.

Figure 7 plots the energy consumption between a random mapping and the optimized energy mapping running on the benchmark applications.

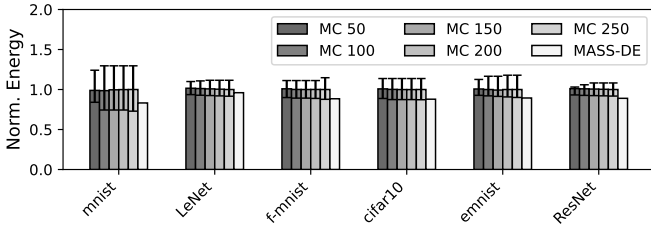


Figure 7: Interconnect energy for different mappings.

On average, energy consumption using our mapping algorithm and cost function is reduced by 13.5% compared to the average values founded using Monte Carlo method. However, the minimum energy consumption founded using Monte Carlo method for mnist application is still lower than the value founded using our algorithm. The reason is because our energy cost function does not take into account spike loss on the network. When spike packets are dropped, the network does not consume dynamic energy for transporting those packets anymore, thus the energy consumption can be lower compared to theoretical cost calculation.

Our algorithm executes significantly faster than the Monte Carlo method when using either the spike loss or energy cost function. Energy mapping outpaces spike loss mapping because the spike loss cost function is more complex compared to the energy cost function.

Models	Monte Carlo	MASS-SL	MASS-DE
mnist	5h 28m 29s	1m 33s	1m 20s
LeNet	8h 45m 12s	3m 10s	1m 57s
f-mnist	15h 55m 03s	38m 26s	3m 44s
cifar10	20h 38m 26s	47m 23s	4m 36s
emnist	22h 12m 50s	1h 03m 39s	5m 30s
ResNet	33h 20m 45s	10h 52m 29s	13m 46s

Table 2: Running time for different mappings.

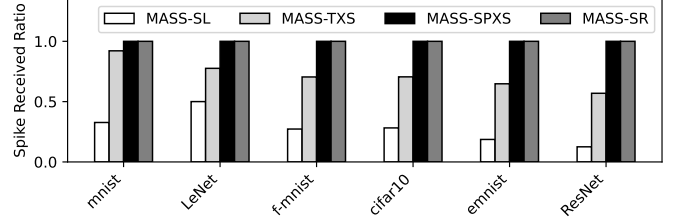


Figure 8: Spike received ratio for non scheduled and scheduled traffic.

5.2. Scheduling and Routing

We compare the trade-off between spike loss and latency for different scheduling options. The scheduling algorithms used here are: MASS-SL (no scheduling), MASS-TXS, MASS-SPXS, and MASS-SR. Figure 8 plots the spike received ratio (the complimentary number of spike loss ratio) and Figure 9 plots the normalized latency for scheduled and non-scheduled traffic running on the benchmark applications.

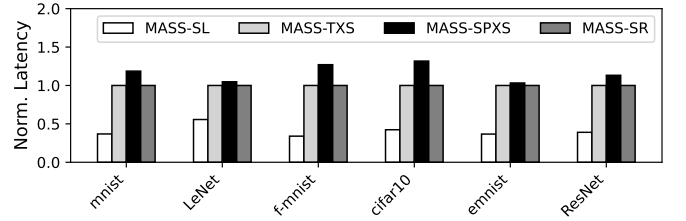


Figure 9: Normalized latency for non scheduled and scheduled traffic.

From these figures, we can clearly see the trade-offs between spike loss and latency using different scheduling options. With no scheduling, the spike loss level is very high at more than 50% while latency remains low. If we spread out the traffic more, the spike loss level can become lower until we achieve zero spike loss with MASS-SPXS. With less spike loss, the energy per spike also reduces as shown in Figure 10. This is because there is less energy wasted for dropping spikes.

With the help of our routing algorithm, MASS-TXS can still be improved upon to provide zero spike loss as shown in the results of MASS-SR. MASS-SR achieves zero spike loss while keeping latency lower than MASS-SPXS and also has a similar level of energy per spike. Hence, it can be concluded that for most spiking neuromorphic applications where spike loss is a crucial metric, we should always choose the MASS-SR option.

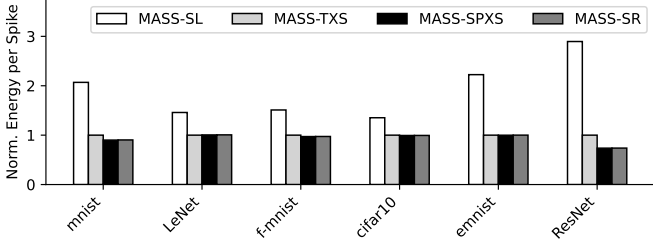


Figure 10: Normalized energy per spike for unscheduled and scheduled traffic.

5.3. Comparison to Other Architectures

In this section, we compare the latency, energy consumption, and energy-delay product (EDP) of four architectures: mesh-based NoC, butterfly NoC, NeuSB, and MASS-SR.

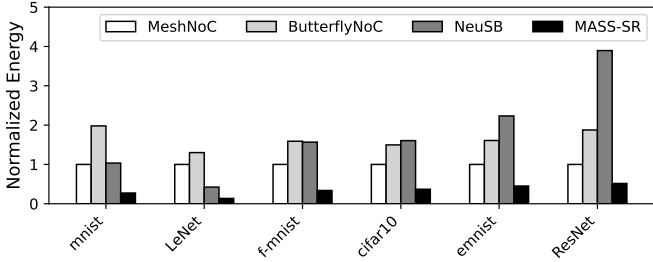


Figure 11: Normalized energy consumption for different architectures.

The main advantage of MASS-SR is its energy efficiency, as shown clearly in Figure 11. Across all applications, MASS-SR consistently consumes the lowest energy compare to all other architectures. On average, MASS-SR consumes 3.48 times less energy than Mesh NoC and 5.47 times less than Butterfly NoC. This is attributed to its lower number of switch counts and bufferless architecture.

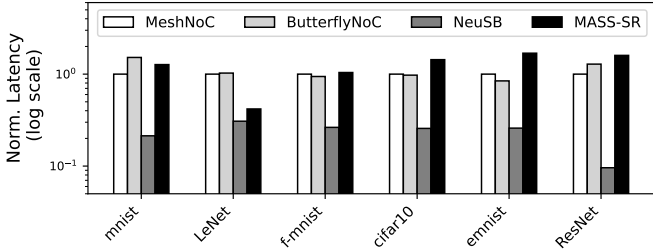


Figure 12: Normalized latency for different architectures.

Figure 12 shows that MASS-SR has a slightly higher latency compared to other architectures due to spike traffic scheduling. On average, MASS-SR experiences a 1.24 times increase in latency compared to Mesh NoC, with a maximum increase of 1.7 times. However, this latency is still negligible for the streaming application domain which we target, where the sample periods are above 1 msec. NeuSB achieves the lowest latency due to its dedicated bus lane per master, which reduces routing complexity and delays.

To assess the balance between latency and energy consumption, we use the energy-delay product (EDP) as a key metric.

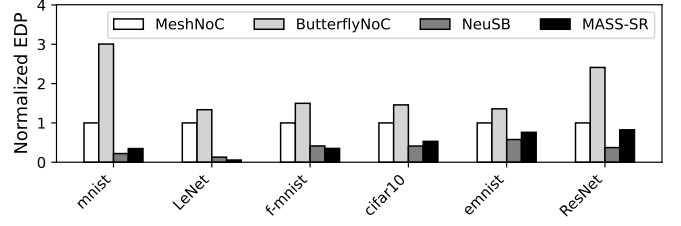


Figure 13: Normalized EDP for different architectures.

Figure 13 illustrates normalized EDP to Mesh NoC for all compared architectures. MASS-SR shows a clear advantage in EDP over traditional NoCs, highlighting its efficient trade-off between latency and energy. Moreover, the design area of MASS is smaller than those of NoCs since there is no memory buffer. While NeuSB achieves a lower EDP than MASS-SR in most applications, this comes at the cost of a larger design area due to its extensive switch requirements. Given the priority of low energy consumption in neuromorphic computing, and the benefits of a compact design, MASS-SR remains the ideal choice for energy-efficient applications.

6. Conclusions

In this work, we introduced MASS, an application mapping framework which is customized for segmented ladder bus architectures. Segmented ladder bus offers highly flexible interconnections, enabling any tile in the system to communicate with another through multiple routing paths. At runtime, this interconnect can establish simultaneous connections based on compile-time communication requirements, making it responsive to the application's dynamic needs. We propose a process for deploying spiking neural network applications on a dynamic segmented bus, designed to minimize spike loss and optimize energy efficiency. This process includes three key steps: cluster mapping, traffic scheduling, and routing. For each step, we develop heuristic algorithms to address the associated challenges effectively.

We conducted a thorough evaluation of MASS on ladder segmented bus in comparison with both NeuSB and traditional NoC architectures using our cycle-accurate network simulator. Simulation results demonstrate that, when compared to conventional NoCs, MASS achieves 3.5 times reduction in energy consumption. Although this reduction comes with a slight increase in delay, this increment is negligible for the application domain which we target, because the speed of the bus is much faster than the communication frequency of the neuron spikes. MASS also offers a clear advantage in EDP over traditional NoCs. This demonstrates its efficient trade-off between latency and energy and makes it well-suited for neuromorphic computing applications.

Acknowledgment

This work is supported by US DOE Award DE-SC0022014 and the US NSF Award CCF-1942697.

References

- [1] N. Rathi, I. Chakraborty, A. Kosta, A. Sengupta, A. Ankit, P. Panda, K. Roy, Exploring neuromorphic computing based on spiking neural networks: Algorithms to hardware, *ACM Computing Surveys* (2023).
- [2] D. S. Modha, F. Akopyan, A. Andreopoulos, et al., Neural inference at the frontier of energy, space, and time, *Science* (2023).
- [3] O. Richter, et al., Dynap-se2: a scalable multi-core dynamic neuromorphic asynchronous spiking neural network processor, *Neuromorphic Computing and Engineering* 4 (1) (2024) 014003.
- [4] M. L. Varshika, A. Balaji, F. Corradi, A. Das, J. Stuijt, F. Catthoor, Design of many-core big little μ Brains for energy-efficient embedded neuromorphic computing, in: *Design, Automation & Test in Europe Conference & Exhibition (DATE)*, 2022.
- [5] B. A. Olshausen, D. J. Field, Sparse coding of sensory inputs, *Current opinion in neurobiology* 14 (4) (2004) 481–487.
- [6] J. Wolfe, A. R. Houweling, M. Brecht, Sparse and powerful cortical spikes, *Current opinion in neurobiology* 20 (3) (2010) 306–312.
- [7] A. Balaji, A. Das, Y. Wu, K. Huynh, F. G. Dell’anna, G. Indiveri, J. L. Krichmar, N. D. Dutt, S. Schaafsma, F. Catthoor, Mapping spiking neural networks to neuromorphic hardware, *IEEE Transactions on Very Large Scale Integration (VLSI) Systems* 28 (1) (2020) 76–86.
- [8] O. Jin, Q. Xing, Y. Li, S. Deng, S. He, G. Pan, Mapping very large scale spiking neuron network to neuromorphic hardware, in: *Proceedings of the 28th ACM International Conference on Architectural Support for Programming Languages and Operating Systems, Volume 3*, 2023, pp. 419–432.
- [9] T. Moscibroda, O. Mutlu, A case for bufferless routing in on-chip networks, in: *ISCA*, 2009.
- [10] G. Michelogiannakis, et al., Evaluating bufferless flow control for on-chip networks, in: *NOCS*, 2010.
- [11] A. Balaji, P. K. Huynh, F. Catthoor, N. D. Dutt, J. L. Krichmar, A. Das, Neusb: A scalable interconnect architecture for spiking neuromorphic hardware, *IEEE Transactions on Emerging Topics in Computing (TETC)* 11 (2) (2023) 373–387. doi:10.1109/TETC.2023.3238708.
- [12] P. K. Huynh, I. Mustafazade, F. Catthoor, N. Kandasamy, A. Das, A scalable dynamic segmented bus interconnect for neuromorphic architectures, *IEEE Embedded Systems Letters* 16 (4) (2024) 505–508. doi:10.1109/LES.2024.3452551.
- [13] P. Raghavan, A. Lambrechts, M. Jayapala, F. Catthoor, D. Verkest, Distributed loop controller for multithreading in unithreaded ilp architectures, *IEEE Transactions on Computers* 58 (3) (2008) 311–321.
- [14] S. Li, S. Guo, L. Zhang, Z. Kang, S. Wang, W. Shi, L. Wang, W. Xu, Sneap: A fast and efficient toolchain for mapping large-scale spiking neural network onto noc-based neuromorphic platform, in: *Proceedings of the 2020 on Great Lakes Symposium on VLSI*, 2020, pp. 9–14.
- [15] C. Xiao, J. Chen, L. Wang, Optimal mapping of spiking neural network to neuromorphic hardware for edge-ai, *Sensors* 22 (19) (2022) 7248.
- [16] I. Mustafazade, N. Kandasamy, A. Das, Clustering and allocation of spiking neural networks on crossbar-based neuromorphic architecture, in: *Proceedings of the 21st ACM International Conference on Computing Frontiers*, 2024, pp. 164–171.
- [17] V. Catania, A. Mineo, et al., Noxim: An open, extensible and cycle-accurate network on chip simulator, in: *ASAP*, 2015.
- [18] Ieee standard for standard systemc® language reference manual, *IEEE Std 1666-2023 (Revision of IEEE Std 1666-2011)* (2023) 1–618doi:10.1109/IEEESTD.2023.10246125.
- [19] M. R. Gary, D. S. Johnson, *Computers and intractability: A guide to the theory of np-completeness* (1979).
- [20] B. Selman, C. P. Gomes, Hill-climbing search, *Encyclopedia of cognitive science* 81 (333-335) (2006) 10.
- [21] L. Niedermeier, K. Chen, J. Xing, et al., Carlsim 6: an open source library for large-scale, biologically detailed spiking neural network simulation, in: *2022 International Joint Conference on Neural Networks (IJCNN)*, IEEE, 2022, pp. 1–10.
- [22] J. K. Eshraghian, M. Ward, E. O. Neftci, X. Wang, G. Lenz, G. Dwivedi, M. Bennamoun, D. S. Jeong, W. D. Lu, Training spiking neural networks using lessons from deep learning, *Proceedings of the IEEE* 111 (9) (2023) 1016–1054. doi:10.1109/JPROC.2023.3308088.
- [23] A. Ekici, Bin packing problem with conflicts and item fragmentation, *Computers & Operations Research* 126 (2021) 105113.
- [24] F. Duchoň, A. Babinec, M. Kajan, P. Beňo, M. Florek, T. Fico, L. Jurišica, Path planning with modified a star algorithm for a mobile robot, *Procedia engineering* 96 (2014) 59–69.
- [25] H. Xiao, K. Rasul, R. Vollgraf, Fashion-mnist: a novel image dataset for benchmarking machine learning algorithms, *arXiv preprint arXiv:1708.07747* (2017).
- [26] G. Cohen, S. Afshar, J. Tapson, A. Van Schaik, Emnist: Extending mnist to handwritten letters, in: *2017 international joint conference on neural networks (IJCNN)*, IEEE, 2017, pp. 2921–2926.
- [27] K. He, X. Zhang, S. Ren, J. Sun, Deep residual learning for image recognition, in: *Proceedings of the IEEE conference on computer vision and pattern recognition*, 2016, pp. 770–778.